

Superconducting fluctuations observed far above T_c in the isotropic superconductor K_3C_{60}

Gregor Jotzu,^{1,*} Guido Meier,¹ Alice Cantaluppi,¹ Andrea Cavalleri,^{1,2}
Daniele Pontiroli,³ Mauro Riccò,³ Arzhang Ardavan,^{2,†} and Moon-Sun Nam^{2,‡}

¹Max Planck Institute for the Structure and Dynamics of Matter, Hamburg, Germany

²Department of Physics, Clarendon Laboratory, University of Oxford, Oxford, UK

³Dipartimento di Scienze Matematiche, Fisiche e Informatiche, Università degli Studi di Parma, Parma, Italy

Alkali-doped fullerides are strongly correlated organic superconductors that exhibit high transition temperatures, exceptionally large critical magnetic fields and a number of other unusual properties. The proximity to a Mott insulating phase is thought to be a crucial ingredient of the underlying physics, and may also affect precursors of superconductivity in the normal state above T_c . We report on the observation of a sizeable magneto-thermoelectric (Nernst) effect in the normal state of K_3C_{60} , which displays the characteristics of superconducting fluctuations. The anomalous Nernst effect emerges from an ordinary quasiparticle background below a temperature of 80K, far above $T_c = 20$ K. At the lowest fields and close to T_c , the scaling of the effect is captured by a model based on Gaussian fluctuations. The temperature up to which we observe fluctuations is exceptionally high for a three-dimensional isotropic system, where fluctuation effects are usually suppressed.

Recent work suggests that the exceptional properties of alkali-doped fulleride superconductors, A_3C_{60} , result from an unusual cooperation between electron-phonon and electron-electron coupling [1–3]. The former is primarily governed by a dynamical Jahn-Teller distortion of the C_{60} molecules leading to an inverted Hund’s coupling between electrons [4], whilst the latter contributes to a suppression of the effective bandwidth. With increasing lattice spacing, superconductivity in A_3C_{60} acquires a “dome-like” T_c , eventually evolving into a Mott insulator with an antiferromagnetic ground state [5, 6]. Unlike other high-temperature superconductors however, A_3C_{60} features no anisotropy, and displays the characteristics of an s-wave superconductor.

A_3C_{60} also seems to follow the Uemura relation [7, 8], with a transition temperature T_c proportional to the superfluid density, suggesting that the loss of long-range phase coherence may be responsible for the disappearance of superconductivity at T_c . Yet, due to the large spread of experimentally determined superfluid densities in A_3C_{60} [9, 10], some uncertainty remains on this assignment.

In K_3C_{60} (see Fig. 1a), observables such as the specific heat and the pressure dependence of T_c suggest that the material may be well described by weak-coupling BCS theory [9, 10], but discrepancies in the size and temperature dependence of the superconducting gap remain [11]. Very recent measurements in few-layer thin films of K_3C_{60} have reported the appearance of a pseudogap up to about twice T_c [12].

Finally, upon illumination with mid-infrared laser pulses, optical properties compatible with superconductivity have been observed in K_3C_{60} at temperatures that

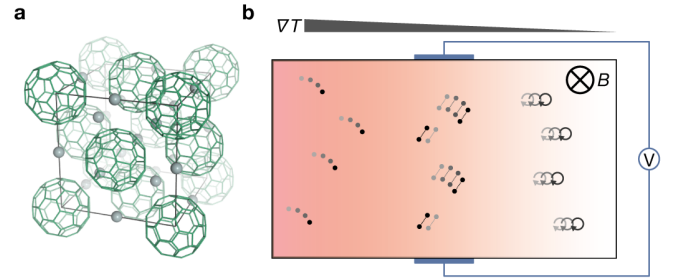


FIG. 1. **Probing the Nernst effect in K_3C_{60} .** **a**, The f.c.c. lattice structure of K_3C_{60} , with potassium atoms shown in grey and carbon buckyballs in green. **b**, Schematic of the measurement configuration. A temperature gradient ∇T is applied orthogonal to the external magnetic field, B . The voltage, V , is then measured orthogonal to both. Cartoons of various possible contributions to the Nernst signal, such as quasiparticles (left), short-lived Cooper pairs (centre) and mobile vortices (right), are included.

exceed T_c by an order of magnitude [13–16], further underscoring a highly unusual normal state. One of the proposed mechanisms for these phenomena suggests that the effect of the light field consists in synchronizing pre-existing, but phase-incoherent, Cooper pairs [15, 17], inspired by the empirical correlation between materials where light-induced high temperature superconductivity can be induced and an anomalous Nernst effect above T_c exists [17–19]. Recent experiments have also provided suggestive magnetic anomalies when Rb_3C_{60} is made to interact with electromagnetic vacuum modes in an optical cavity [20].

The Nernst effect describes the appearance of an electric field, $E_y = -e_N \partial_x T$, transverse to an applied temperature gradient, $\partial_x T$, and to a magnetic field B_z pointing along the third spatial direction. The Nernst signal e_N is related to the conductivity and thermoelectric ten-

* gregor.jotzu@mpsd.mpg.de

† arzhang.ardavan@physics.ox.ac.uk

‡ moon-sun.nam@physics.ox.ac.uk

sors, σ and α via

$$e_N = \frac{\alpha_{xy}\sigma_{xx} - \alpha_{xx}\sigma_{xy}}{\sigma_{xx}^2 + \sigma_{xy}^2} \approx \frac{\alpha_{xy}}{\sigma_{xx}} - S\mu_H B_z \quad (1)$$

for an isotropic system. $\mu_H = \sigma_{xy}/\sigma_{xx}B_z$ denotes the Hall mobility and $S = \alpha_{xx}/\sigma_{xx}$ the Seebeck coefficient. The approximate equality holds for small Hall angles, and is an excellent approximation for the parameters used in this work.

For a metal, the effect can be seen as a combination of a flow of charges carrying entropy along a temperature gradient, the Seebeck effect, and the deflection of moving charges in the presence of a magnetic field, the Hall effect (see Fig. 1b). However, with exact particle-hole symmetry, the two terms in Eq. 1 would cancel exactly [21]. The overall sign and amplitude of the effect will depend on the details of the quasiparticle band structure, which the Nernst signal is therefore very sensitive to. In the free-electron approximation, this signal is linear in temperature.

In a superconductor, a different contribution to the Nernst effect arises from the movement of superconducting vortices. When these mobile vortices carry entropy along the applied temperature gradient (see Fig. 1b), they also carry magnetic flux, which induces a voltage in the transverse direction [22, 23]. This effect is much larger than its metallic counterpart, and shows a highly non-linear dependence on B_z , perhaps owing to a competition between vortex density and vortex mobility.

If, at T_c , superconducting long-range order breaks down because of fluctuations of the phase of the order parameter, while a finite Cooper pair amplitude remains, this vortex Nernst effect would be expected to survive at temperatures above T_c . However, even for a transition driven by a thermal breakdown of Cooper pairing, the thermal diffusion of short-lived Cooper pairs may also contribute to the Nernst signal above T_c [22, 24, 25].

In general, the presence of such precursors of superconductivity is expected to be suppressed as the dimensionality of the system increases. Indeed, Nernst signals that could be related to superconducting precursors have been reported in layered and thin-film samples [18, 22, 25–27], but we are not aware of any previous observations in an isotropic three-dimensional system. Interestingly, K_3C_{60} and Rb_3C_{60} were the first fully three-dimensional materials where slight deviations of the normal state conductivity in the immediate vicinity of T_c could be attributed to paraconductivity [28].

In the experiments reported in this paper, air-sensitive K_3C_{60} powders were compressed into pellets and incorporated into a circuit board printed on an FR4 substrate, which features low thermal conductivity. Embedded heaters and temperature sensors, as well as indium-coated contacts with contact resistances below 1 Ohm were used to optimize these measurements (see Appendix and Fig. S1). Four-probe resistance measurements (see Appendix) were used to identify the superconducting transition, as shown in the inset of Fig. 2a. In zero

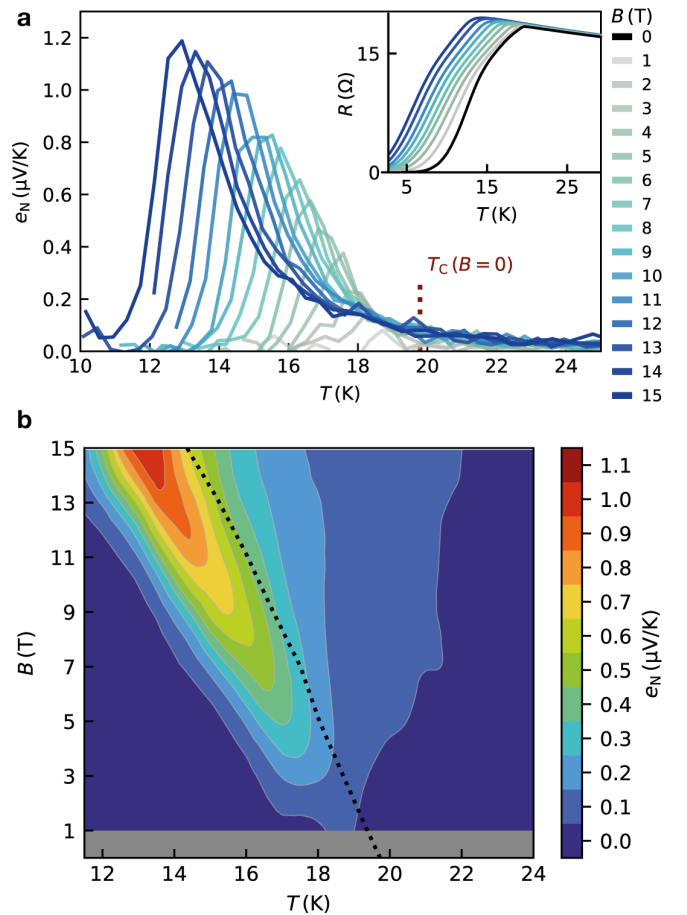


FIG. 2. **Nernst signal in the superconducting regime.** **a**, Measured transverse thermoelectric effect, e_N , in the presence of magnetic fields ranging from 1T (grey line) to 15T (blue line), in steps of 1T. The red dashed line shows the critical temperature in zero field. Inset: Sample resistance near the critical temperature, 0T (black) to 15T (blue) range. **b**, Contour plot of e_N as a function of temperature and magnetic field. The black dotted line shows the resistive $T_c(B)$. A Gaussian convolution was used for smoothing, and in the low-T, low-B region the data was sparse and was interpolated. See Fig. S3b for raw data and the field-normalized e_N/B .

field, we found $T_c(B = 0) = 19.8\text{K}$, in good agreement with previous reports and with magnetic measurements on the same batch of samples [9, 10, 14]. A Werthamer-Helfand-Hohenberg theory [29] was used to extrapolate the zero-temperature upper critical field, $\mu_0 H_{c2}(0)$, from the field dependence of the resistive transition via: $\mu_0 H_{c2}(0) = 0.69\mu_0 T_c \left. \frac{\partial H_{c2}}{\partial T} \right|_{T_c}$, where μ_0 denotes the vacuum permeability. This yielded a value of about 39T, corresponding to a zero-temperature coherence length of $\xi_0 = \sqrt{\Phi_0/2\pi\mu_0 H_{c2}(0)} = 2.9\text{nm}$ (here Φ_0 is the magnetic flux quantum). This lies within the range of values extrapolated from other experiments [9, 10], and closely matches the value recently determined using pulsed fields in a range exceeding H_{c2} [30].

As expected, no Nernst signal (e_N) was observed for temperatures far below T_c , likely due to freezing of vortex motion. For higher temperatures, entering the temperature range where vortices become mobile, the signal was seen to increase (see Fig. 2a). For a given magnetic field, the number of vortices in the system remains nearly constant (as all fields in our measurements were much larger than the lower critical field), but their mobility increases rapidly. Near T_c , the Nernst signal reduced again. A detailed quantitative understanding of this well-known phenomenon is still lacking – both the increasing vortex-vortex interactions that appear as vortex length scales increase, as well as a change in the entropy per vortex are relevant [22, 31]. Although the amplitude of e_N did not saturate at the largest applied field, the value it approaches agrees with an upper bound that was found to apply to various superconductors spanning several orders of magnitude in critical fields and temperatures [32].

The Nernst signal as a function of magnetic field (see Fig. S3a) peaked at a field B_{\max} , that reduces on approaching the critical temperature. This reduction fits very well to a linear function with a slope of $-2.27(3)$ T/K, see Fig. 3c. It displays a zero-field intersect at $T = 19.5(1)$ K, close to the resistive critical temperature $T_c(B = 0) = 19.8$ K. B_{\max} has previously been shown to bear some similarity to a softening mode [22, 33], and its vanishing value when approaching $T_c(0)$ suggests that the Nernst effect changes in nature when crossing T_c .

Above T_c , precursors of superconductivity may contribute to the Nernst signal, but quasiparticles can also play a role. The latter contribution is expected to scale linearly with magnetic field and temperature (at constant volume) for a simple metallic state. [21] We therefore used the temperature- and magnetic-field-normalized Nernst coefficient, $\mathcal{N} = e_N/BT$, in order to detect anomalous behaviour. In Fig. 3a, \mathcal{N} is shown to evolve smoothly across T_c , remaining positive and retaining a strong field dependence, as expected for a signal that is primarily caused by superconducting fluctuations. The inset in Fig. 3a shows that \mathcal{N} displays near-universal behaviour upon approaching the field-dependent critical temperature, $T_c(B)$, (see also Fig. S3d).

At higher temperatures, we observed two characteristic features in the data (see Fig. 3b): First, at $T_0(B) \approx 50$ K, the signal changed from positive to negative. The temperature of the zero-crossing, $T_0(B)$, shows a similar field dependence as $T_c(B)$, (see Fig. 3c). Second, a minimum in \mathcal{N} appears at $T_{\min}(B) \approx 80$ K, above which \mathcal{N} shows a linear and positive slope.

In order to disentangle the superconducting contribution to \mathcal{N} we first focus on the high-temperature limit, where the quasiparticle contribution should become dominant. We can compare the behaviour of \mathcal{N} in this regime to the expected signal in a single band free-electron model of a metal. There, $|\mathcal{N}| \sim \mu_H S/T$, with a pre-factor of order unity [21]. This relationship implies that the Nernst effect is proportional to the ratio of the mobility and the

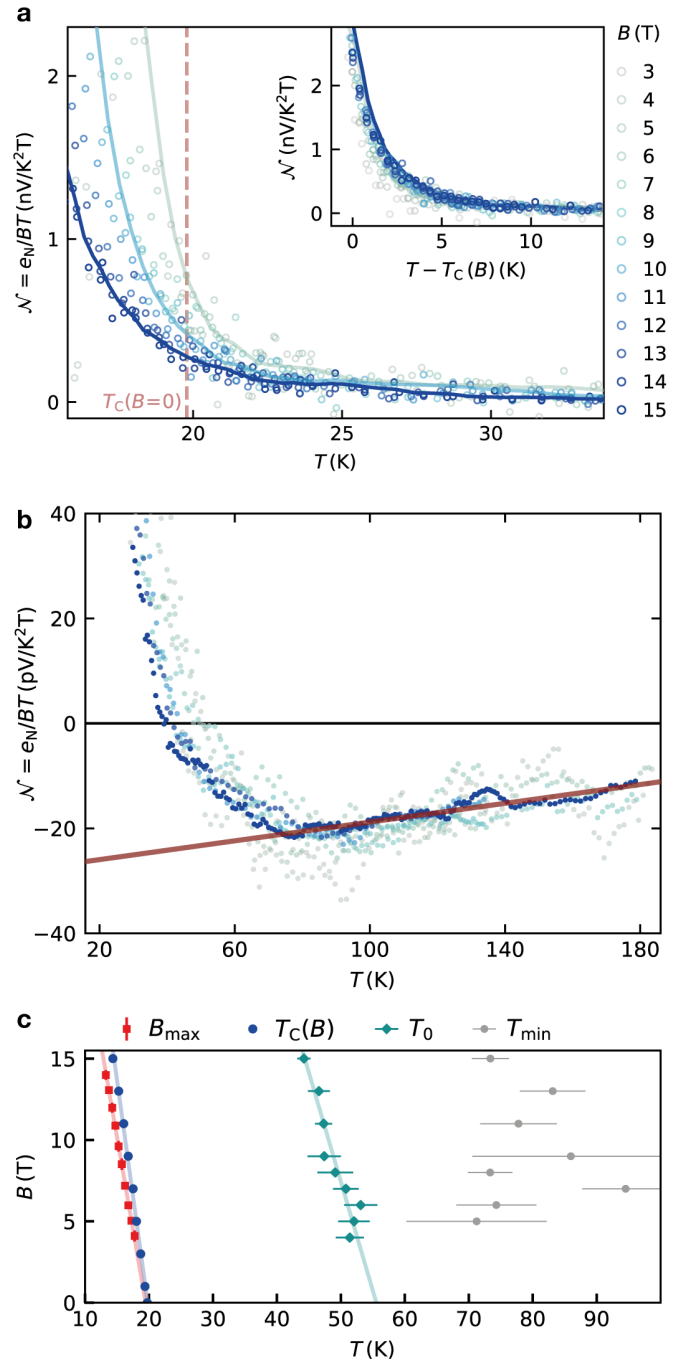


FIG. 3. **Anomalous Nernst effect above T_c .** **a**, Nernst coefficient \mathcal{N} close to T_c (red dashed line). Open symbols show the raw data, lines are 10-point boxcar averages for 5T, 10T and 15T (grey to blue). Inset: Same data re-scaled with the field-dependent $T_c(B)$. **b**, \mathcal{N} at higher temperatures, after 10-point boxcar averaging (Note the reduced y -scale). The red curve corresponds to the quasiparticle contribution $-2.7\mu_H S/T$. **c**, Characteristic quantities extracted from the Nernst signal: B_{\max} denotes the fitted peak of $e_N(B)$ (see Fig. 2b), T_0 and T_{\min} are the zero-crossing and minimum of \mathcal{N} , respectively. T_c denotes the resistive superconducting transition temperature. All lines are linear fits. Error bars indicate fit uncertainties.

Fermi energy in the metal, which was found to hold in a variety of materials, with \mathcal{N} ranging from $1\text{mV}/\text{K}^2\text{T}$ down to $1\text{nV}/\text{K}^2\text{T}$ [22]. We use previously determined values for the T -linear S and μ_{H} [34, 35], where the latter shows a linear dependence on temperature that has been shown to scale with the expansion of the lattice. As shown in Fig. 3b, we find excellent agreement with our data above T_{min} , using a quasiparticle contribution of $-2.7\mu_{\text{H}}S/T$, and no significant field-dependence of \mathcal{N} . Given the complex band structure of K_3C_{60} , the agreement with such a simple scaling is remarkable. It extends its range of validity to values of \mathcal{N} which are two orders of magnitude smaller than those reported so far [22].

The rapid change in the slope of \mathcal{N} signals a significant change in the electronic properties of the material. Such a change could for example be caused by the appearance of charge-density wave order [36], and in a number of cuprate superconductors a very similar feature was found to coincide closely with the pseudogap temperature T^* [27]. In K_3C_{60} , a transition to a frozen orientational disorder of the C_{60} molecules is known to occur, but at a temperature very close to 200K [37, 38]. There are no observations pointing at the appearance of competing orders around 80K , although it is worth noting that a certain deviation from linearity has been observed in the Seebeck effect, which has been attributed to electron-phonon coupling or precursors of superconductivity [34, 39, 40].

An effect related to the superconducting ground state seems much more likely, given that the magnetic field dependence of \mathcal{N} tracks $T_c(B)$. In the following we will consider two scenarios through which precursors of superconductivity could cause such an upturn in \mathcal{N} : a vortex-based Nernst signal surviving in a phase-fluctuating regime above T_c , or a signal caused by short-lived Cooper pairs.

For the latter scenario, a theory based on Gaussian fluctuations in a Ginzburg-Landau model [24] predicts a superconducting contribution, $e_{\text{N}}^{\text{SCG}}$, to the Nernst signal given by:

$$\frac{e_{\text{N}}^{\text{SCG}}}{B_z} = \frac{\alpha_{xy}^{\text{SCG}}}{\sigma_{xx} B_z} = \frac{k_{\text{B}} e^2}{12\pi \hbar^2} \frac{\xi}{\sigma_{xx}} \quad (2)$$

with

$$\xi = \frac{\xi_0}{\sqrt{\epsilon}} = \frac{\xi_0}{\sqrt{(T - T_c)/T_c}} \quad (3)$$

for a three-dimensional system, where e is the electron charge and \hbar the reduced Planck constant. The two-dimensional version of this theory is in good agreement with measurements on conventional [22, 25] and some unconventional [33, 41] superconductors. Its prediction of a field-independent Nernst coefficient applies to the low-field regime, where the coherence length ξ is short compared to the magnetic length $l_B = \sqrt{\hbar/eB}$, and $T_c(B) \approx T_c(0)$. As it is a continuum theory, it may also become invalid once ξ becomes as short as the lattice

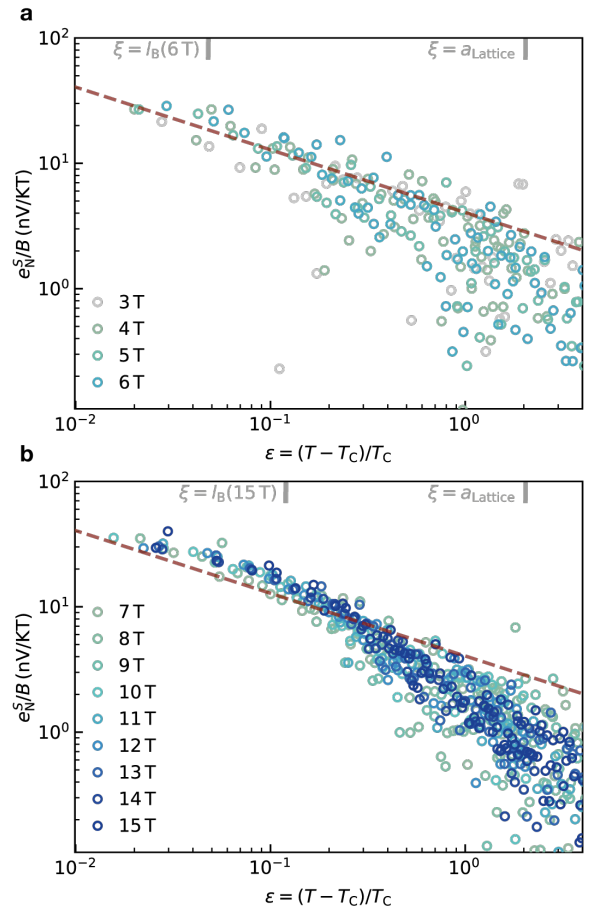


FIG. 4. **Scaling of the superconducting Nernst coefficient $e_{\text{N}}^{\text{S}}/B$ above T_c .** **a**, Quasiparticle-subtracted contribution to the Nernst coefficient, $e_{\text{N}}^{\text{S}}/B = e_{\text{N}}/B + 2.7\mu_{\text{H}}S$, for magnetic fields between 3T and 6T. Color scale as in Fig. 1. The data are shown as a function of the distance to the field-dependent critical temperature at zero field. **b**, Data for higher fields, up to 15T. The dashed red line shows the expected low-field value from a model based on Gaussian fluctuations, with a constant conductivity of $6(\text{m}\Omega\text{cm})^{-1}$ (see text). The top axes indicate where the coherence length, ξ , becomes equal to the lattice spacing, a_{Lattice} , or to the magnetic length l_B at the highest field shown in the respective panel.

spacing, and generally speaking Ginzburg-Landau theory is only applicable in the vicinity of T_c .

In Fig. 4a, we compare our measurements for fields up to 6T to this theory by subtracting the fitted quasiparticle contribution determined above (red line in Fig. 3b) from the measured Nernst signal. See Fig. S2 for other possible subtraction schemes. We find that the data is overall well described by the simple $1/\sqrt{\epsilon}$ scaling predicted by theory if we use a conductivity of $6(\text{m}\Omega\text{cm})^{-1}$. Although we expect our measurement to be sensitive to the intrinsic conductivity, rather than grain boundary effects [42], this value is still about three times larger than the conductivity of high-purity single crystals. [9] Interestingly however, a very similar discrepancy was found

in measurements of the paraconductivity [28], suggesting that the residual conductivity describing the transport properties of superconducting fluctuations may not be identical to the one extracted from direct measurements.

At higher temperatures, beyond the expected regime of validity of this model, deviations from the simple scaling occur, which might be captured by perturbative expansions [43, 44]. Interestingly, at higher fields (see Fig. 4b), the behaviour does not follow a single power law. This suggests that in high field, the resistive $T_c(B)$ deviates from the thermodynamical critical point, which is a characteristic of unconventional superconductors [45].

In order to gauge the plausibility of a phase-fluctuating scenario, we use the framework proposed by Emery and Kivelson [46] to estimate the temperature T_θ at which global phase coherence in the superconductor would be destroyed by thermal fluctuations – even if pairing were to survive up to a higher “mean field temperature” T_{MF} . Taking the most recent (and largest) value for the penetration depth in K_3C_{60} , $\lambda = 890\text{nm}$ [47], we find a temperature T_θ as low as 80K. This is only 4 times larger than T_c , whereas for conventional superconductors T_θ/T_{MF} can be on the order of 10^5 . Additionally, by taking into account some degree of quantum fluctuations (as expected given the relative proximity of a Mott-insulating state), it would be possible that the superconducting transition is somewhat suppressed below T_{MF} .

We are not aware of a quantitative prediction of the vortex Nernst signal above T_c in a three-dimensional system. Results in two dimensions [31] suggest an important role of the lattice geometry, and can therefore not simply be extrapolated to our system. As the difference between mean-field models and fully quantum-mechanical descriptions becomes less pronounced in higher dimensions, small deviations at high temperatures and magnetic field may play a key role in distinguishing different scenarios. Our data therefore also provide an important benchmark for a theoretical framework describing the appearance of light-induced superconductivity in K_3C_{60} based on the synchronization of stable but globally phase-incoherent Cooper pairs, which would also have to correctly describe the initial static state.

It would be highly interesting to extend our work to Rb_3C_{60} and especially $Rb_xCs_{3-x}C_{60}$, where quantum phase fluctuations caused by the proximity of the Mott-insulating state will be enhanced. For the latter family, a suppression in T_c upon approaching the quantum phase transition has been observed [5, 6], but could not be reproduced in an otherwise quantitatively successful theoretical model [1]. Studying the Nernst effect in this regime, which should be possible using the experimental framework presented here, would provide new insights concerning the nature of the superconducting transition in the fullerenes, and of phase-incoherent superconductivity in general.

Acknowledgements We thank Michele Buzzi, Dante Kennes, Daniel Podolsky and Dharmalingam Prab-

akaran for insightful discussions, and Boris Fiedler for superb technical assistance.

APPENDIX

Appendix A: Sample preparation

The K_3C_{60} powder used in this work was prepared and characterized as previously reported in Refs. [13–15]. In brief, finely ground C_{60} powder and metallic potassium were placed in a vessel inside a Pyrex vial in stoichiometric amounts, evacuated to 10^{-6}mbar , and sealed. The two materials were heated at 523K for 72h and then at 623K for 28h, and kept separated to ensure that the C_{60} was only exposed to clean potassium vapour. After regrinding and pelletizing in an inert Ar atmosphere, the sample was annealed at 623K for 5 days. Powder X-ray diffraction measurements confirmed the purity of K_3C_{60} and indicated a grain size between 100nm and 400nm. Magnetic susceptibility measurements yielded a T_c of 19.8K [13]. For the Nernst effect and 4-point resistivity measurements the sample was handled inside an Ar glove box with $<0.2\text{ppm}$ O_2 and H_2O . It was placed inside an FR4-frame, which had been glued to the circuit board described below using thermally and electrically insulating, minimally-outgassing glue (Epo-TeK 301-2FL-T), see Fig. S1. The powder was then compressed with an FR4 piston, and sealed with the same glue. The resistance of the sample was monitored to ensure that no contamination occurred during the sealing process and the subsequent transfer to the cryostat.

Appendix B: Nernst effect measurement setup

We used a printed copper circuit board on an FR4 substrate (which features a low thermal conductivity, $\sim 0.1\text{W/Km}$ at 10K [48]), as shown in Fig. S1b. Cernox temperature sensors were embedded in thermally conductive glue (Stycast 2850FT) in milled pockets on each side of the sample. They were used to monitor the temperature gradient across the sample, which was induced using a resistive heater. An additional Cernox sensor was attached to the bottom of the circuit board to monitor the base temperature. The circuit board was mounted to the cold finger of a cryostat using non-magnetic (titanium) screws and spring washers, and PMMA spacers were used for additional thermal insulation. In the sample compartment, the copper contacts were coated with indium, yielding contact resistances below 1 Ohm. The transverse voltage was measured whilst slowly cooling the sample. Data for opposite magnetic fields (see Fig. S1c), was then subtracted to compute the Nernst signal.

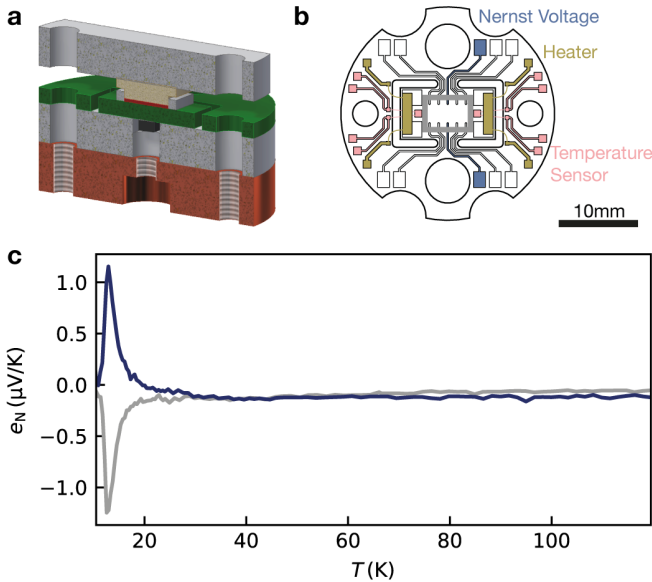


FIG. S1. **Experimental setup.** **a**, The sample (red) is pressed on top of a circuit board (green) using a PMMA piston (beige). The sample space is encapsulated using non-conductive epoxy glue. The base temperature is measured with a sensor (black) pressed against the bottom of the circuit board. The sample and circuit board are mounted on the cold finger of a cryostat (copper) using titanium screws (not shown), using spacers made of PMMA (grey). **b**, Schematic of the circuit board. The sample compartment is indicated by a grey rectangle. A temperature sensor is placed on each side of the sample in a milled pocket, encapsulated by thermally-conductive epoxy glue. Resistive heaters are placed on each side. The Nernst signal is measured with the indicated indium-coated contacts in the centre of the sample compartment. The other contacts are used for four-point resistance measurements. **c**, Transverse voltage at +15T (blue) and -15T (grey). For the data shown in the main text, the Nernst signal was evaluated as half of the difference between signals measured at opposite fields.

Appendix C: Resistance measurements

The resistance of the sample was determined using a low-frequency lock-in measurement in a linear 4-contact configuration, with contacts as shown in Fig. S1b. Above T_c , the sample showed an increase in resistance upon cooling, as previously observed in granular K_3C_{60} samples [9, 10]. In order to determine T_c , the point at which the resistance changes slope was used, which yielded a zero-field T_c consistent with magnetic susceptibility measurements on the same batch of sample. We verified that the width of the transition is not sensitive to reducing the probe current below the value of $2\mu A$ which we used.

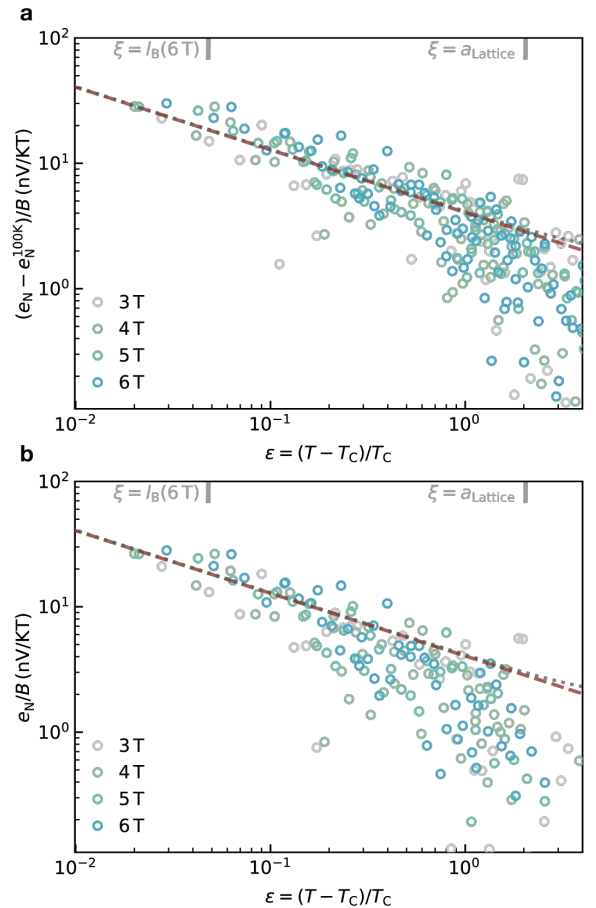


FIG. S2. **Effect of subtracting the quasiparticle signal on the scaling analysis.** **a**, Same as Fig. 4a, but subtracting the fixed value of e_N/B at 100K instead of a temperature-dependent function. The grey dotted line shows the theoretical prediction of Eq. 2, but using a quadratic temperature dependence for the conductivity. **b**, The Nernst coefficient e_N/B without any subtraction of the quasiparticle contribution. Note that this results in some negative values for e_N at higher temperatures, which do not appear in this logarithmic plot.

Appendix D: Subtraction of the quasiparticle signal

We verify that the details of how the quasiparticle contribution to e_N is subtracted do not strongly affect the comparison to the Gaussian fluctuation model shown in Fig. 3, by comparing different subtraction schemes: In Fig. S3a, instead of subtracting the temperature-dependent quasiparticle function ($-2.7\mu_H S$), we subtract its fixed value at 100K. Here, the simple theoretical model seems to capture the data even at higher temperatures. In Fig. S3b, we plot e_N without any quasi-particle subtraction. This leads to a deviation at high temperatures (as expected given that the signal changes sign there), but within the expected range of the validity of the theoretical model, it still captures the data well. We have also

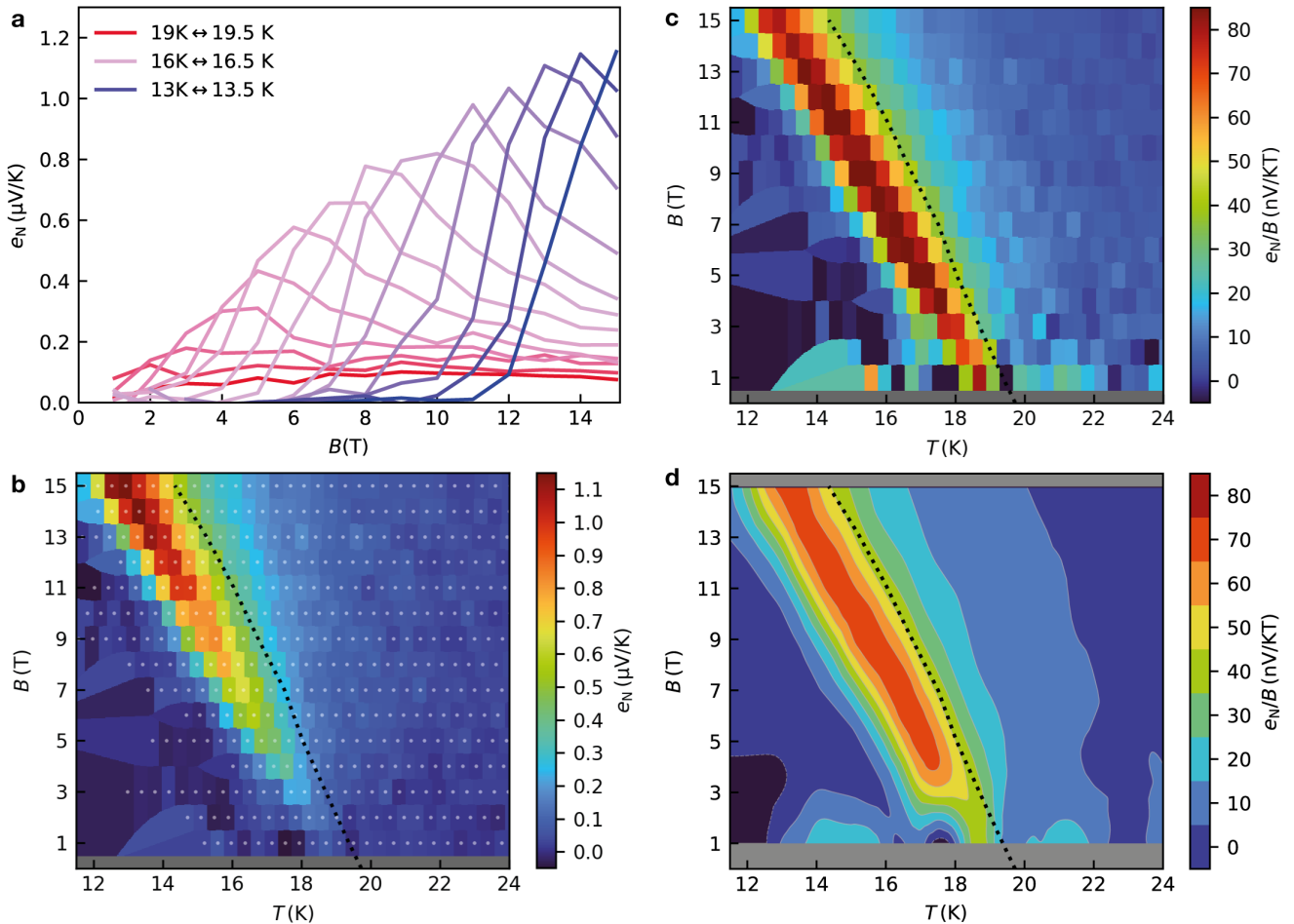


FIG. S3. **B-T maps of the Nernst signal.** **a**, e_N as a function of magnetic field for different temperatures below $T_c(B)$. **b**, Raw data of e_N as a function of temperature and magnetic field (see Fig. 2 for a smoothed contour map). Grey dots indicate the B-T values of each measurements, the data is interpolated to the nearest available point. The black dotted line shows $T_c(B)$. **c**, Same as (b), but showing the field-normalized value e_N/B . **d**, Smoothed contour plot of (c).

verified that using a temperature-dependent value of the conductivity in Eq. 2 (where we have used the quadratic

dependence found in [49] as a comparison), has a negligible effect in the relevant range.

-
- [1] Y. Nomura, S. Sakai, M. Capone, and R. Arita, *Exotic s-wave superconductivity in alkali-doped fullerenes*, *Journal of Physics: Condensed Matter* **28**, 153001 (2016).
- [2] M. Capone, M. Fabrizio, C. Castellani, and E. Tosatti, *Strongly correlated superconductivity*, *Science* **296**, 2364 (2002).
- [3] S. Chakravarty, M. P. Gelfand, and S. Kivelson, *Electronic correlation effects and superconductivity in doped fullerenes*, *Science* **254**, 970 (1991).
- [4] Phonon effects may not necessarily be required for an inverted Hund's coupling, see H.-C. Jiang and S. Kivelson, *Electronic pair binding and Hund's rule violations in doped C_{60}* , *Physical Review B* **93**, 165406 (2016).
- [5] Y. Takabayashi, A. Y. Ganin, P. Jeglič, D. Arčon, T. Takano, Y. Iwasa, Y. Ohishi, M. Takata, N. Takeshita, K. Prassides, and M. J. Rosseinsky, *The Disorder-Free Non-BCS Superconductor Cs_3C_{60} Emerges from an Antiferromagnetic Insulator Parent State*, *Science* **323**, 1585 (2009).
- [6] R. H. Zadik, Y. Takabayashi, G. Klupp, R. H. Colman, A. Y. Ganin, A. Potočnik, P. Jeglič, D. Arčon, P. Matius, K. Kamarás, Y. Kasahara, Y. Iwasa, A. N. Fitch, Y. Ohishi, G. Garbarino, K. Kato, M. J. Rosseinsky, and K. Prassides, *Optimized unconventional superconductivity in a molecular Jahn-Teller metal*, *Science Advances* **1**, e1500059 (2015).
- [7] Y. Uemura, A. Keren, L. Le, G. Luke, W. Wu, J. Tsai, K. Tanigaki, K. Holczer, S. Donovan, and R. Whetten, *System dependence of the magnetic-field penetration depth in C_{60} superconductors*, *Physica C: Superconductivity* **235-240**, 2501 (1994).

- [8] Y. J. Uemura, G. M. Luke, B. J. Sternlieb, J. H. Brewer, J. F. Carolan, W. N. Hardy, R. Kadono, J. R. Kempton, R. F. Kiefl, S. R. Kreitzman, P. Mulhern, T. M. Rise- man, D. L. Williams, B. X. Yang, S. Uchida, H. Takagi, J. Gopalakrishnan, A. W. Sleight, M. A. Subramanian, C. L. Chien, M. Z. Cieplak, G. Xiao, V. Y. Lee, B. W. Statt, C. E. Stronach, W. J. Kossler, and X. H. Yu, *Universal Correlations between T_c and n_s/m^* (Carrier Density over Effective Mass) in High- T_c Cuprate Superconductors*, *Physical Review Letters* **62**, 2317 (1989).
- [9] O. Gunnarsson, *Alkali-Doped Fullerenes: Narrow-Band Solids With Unusual Properties* (World Scientific, 2004).
- [10] K. M. Kadish and R. S. Ruoff, *Fullerenes: Chemistry, Physics, and Technology* (John Wiley & Sons, 2000).
- [11] C. M. Lieber and Z. Zhang, *Physical properties of metal-doped fullerene superconductors*, *Solid State Physics* **48**, 349 (1994).
- [12] M.-Q. Ren, S. Han, S.-Z. Wang, J.-Q. Fan, C.-L. Song, X.-C. Ma, and Q.-K. Xue, *Direct Observation of Full-Gap Superconductivity and Pseudogap in Two-Dimensional Fullerenes*, *Physical Review Letters* **124**, 187001 (2020).
- [13] M. Mitrano, A. Cantaluppi, D. Nicoletti, S. Kaiser, A. Perucchi, S. Lupi, P. Di Pietro, D. Pontiroli, M. Riccò, and S. R. Clark, *Possible light-induced superconductivity in K_3C_{60} at high temperature*, *Nature* **530**, 461 (2016).
- [14] A. Cantaluppi, M. Buzzi, G. Jotzu, D. Nicoletti, M. Mitrano, D. Pontiroli, M. Riccò, A. Perucchi, P. Di Pietro, and A. Cavalleri, *Pressure tuning of light-induced superconductivity in K_3C_{60}* , *Nature Physics* **14**, 837 (2018).
- [15] M. Budden, T. Gebert, M. Buzzi, G. Jotzu, E. Wang, T. Matsuyama, G. Meier, Y. Laplace, D. Pontiroli, M. Riccò, F. Schlawin, D. Jaksch, and A. Cavalleri, *Evidence for metastable photo-induced superconductivity in K_3C_{60}* , *Nature Physics* **17**, 611 (2021).
- [16] M. Buzzi, G. Jotzu, A. Cavalleri, J. I. Cirac, E. A. Demler, B. I. Halperin, M. D. Lukin, T. Shi, Y. Wang, and D. Podolsky, *Higgs-mediated optical amplification in a nonequilibrium superconductor*, *Physical Review X* **11**, 011055 (2021).
- [17] Y. J. Uemura, *Dynamic superconductivity responses in photoexcited optical conductivity and Nernst effect*, *Physical Review Materials* **3**, 104801 (2019).
- [18] M.-S. Nam, A. Ardavan, S. J. Blundell, and J. A. Schlueter, *Fluctuating superconductivity in organic molecular metals close to the Mott transition*, *Nature* **449**, 584 (2007).
- [19] M. Buzzi, D. Nicoletti, M. Fechner, N. Tancogne-Dejean, M. A. Sentef, A. Georges, T. Biesner, E. Uykur, M. Dres- sel, and A. Henderson, *Photomolecular high-temperature superconductivity*, *Physical Review X* **10**, 031028 (2020).
- [20] A. Thomas, E. Devaux, K. Nagarajan, T. Chervy, M. Seidel, D. Hagenmüller, S. Schütz, J. Schachenmayer, C. Genet, G. Pupillo, and T. W. Ebbesen, *Exploring Superconductivity under Strong Coupling with the Vacuum Electromagnetic Field*, arXiv:1911.01459 (2019).
- [21] K. Behnia, *The Nernst effect and the boundaries of the Fermi liquid picture*, *Journal of Physics: Condensed Matter* **21**, 113101 (2009).
- [22] K. Behnia and H. Aubin, *Nernst effect in metals and superconductors: A review of concepts and experiments*, *Reports on Progress in Physics* **79**, 046502 (2016).
- [23] An additional contribution from the Magnus force is also present, see V. Krasnov and G. Y. Logvenov, *Selfcon- sistent analysis of magnus and thermal forces acting on vortices in type-ii superconductors*, *Physica C: Supercon- ductivity* **274**, 286 (1997).
- [24] I. Ussishkin, S. L. Sondhi, and D. A. Huse, *Gaussian Superconducting Fluctuations, Thermal Transport, and the Nernst Effect*, *Physical Review Letters* **89**, 287001 (2002).
- [25] A. Pourret, H. Aubin, J. Lesueur, C. A. Marrache- Kikuchi, L. Bergé, L. Dumoulin, and K. Behnia, *Observation of the Nernst signal generated by fluctuating Cooper pairs*, *Nature Physics* **2**, 683 (2006).
- [26] N. Ong, Y. Wang, S. Ono, Y. Ando, and S. Uchida, *Vorticity and the Nernst effect in cuprate superconductors*, *Annalen der Physik* **13**, 9 (2004).
- [27] O. Cyr-Choinière, R. Daou, F. Laliberté, C. Collignon, S. Badoux, D. LeBoeuf, J. Chang, B. J. Ramshaw, D. A. Bonn, W. N. Hardy, R. Liang, J.-Q. Yan, J.-G. Cheng, J.-S. Zhou, J. B. Goodenough, S. Pyon, T. Takayama, H. Takagi, N. Doiron-Leyraud, and L. Taillefer, *Pseudo- gap temperature T^* of cuprate superconductors from the Nernst effect*, *Physical Review B* **97**, 064502 (2018).
- [28] X.-D. Xiang, J. G. Hou, V. H. Crespi, A. Zettl, and M. L. Cohen, *Three-dimensional fluctuation conductivity in su- perconducting single crystal K_3C_{60} and Rb_3C_{60}* , *Nature* **361**, 54 (1993).
- [29] N. R. Werthamer, E. Helfand, and P. C. Hohenberg, *Tem- perature and purity dependence of the superconducting critical field, H_{c2} . III. Electron spin and spin-orbit ef- fects*, *Physical Review* **147**, 295 (1966).
- [30] Y. Kasahara, Y. Takeuchi, R. H. Zadik, Y. Takabayashi, R. H. Colman, R. D. McDonald, M. J. Rosseinsky, K. Prassides, and Y. Iwasa, *Upper critical field reaches 90 Tesla near the Mott transition in fulleride supercon- ductors*, *Nature Communications* **8**, 14467 (2017).
- [31] D. Podolsky, S. Raghu, and A. Vishwanath, *Nernst Ef- fect and Diamagnetism in Phase Fluctuating Supercon- ductors*, *Physical Review Letters* **99**, 117004 (2007).
- [32] C. W. Rischau, Y. Li, B. Fauqué, H. Inoue, M. Kim, C. Bell, H. Y. Hwang, A. Kapitulnik, and K. Behnia, *Universal Bound to the Amplitude of the Vortex Nernst Signal in Superconductors*, *Physical Review Letters* **126**, 077001 (2021).
- [33] F. F. Tafti, F. Laliberté, M. Dion, J. Gaudet, P. Fournier, and L. Taillefer, *Nernst effect in the electron-doped cuprate superconductor $Pr_{2-x}Ce_xCuO_4$: Superconducting fluctuations, upper critical field H_{c2} , and the origin of the T_c dome*, *Physical Review B* **90**, 024519 (2014).
- [34] T. Inabe, H. Ogata, Y. Maruyama, Y. Achiba, S. Suzuki, K. Kikuchi, and I. Ikemoto, *Electronic structure of alkali metal doped C_{60} derived from thermoelectric power mea- surements*, *Physical Review Letters* **69**, 3797 (1992).
- [35] L. Lu, V. H. Crespi, M. S. Fuhrer, A. Zettl, and M. L. Cohen, *Universal Form of Hall Coefficient in K and Rb Doped Single Crystal C_{60}* , *Physical Review Letters* **74**, 1637 (1995).
- [36] R. Bel, K. Behnia, and H. Berger, *Ambipolar Nernst Ef- fect in $NbSe_2$* , *Physical Review Letters* **91**, 066602 (2003).
- [37] Y. Yoshinari, H. Alloul, G. Kriza, and K. Holczer, *Molec- ular dynamics in K_3C_{60} : A C^{13} NMR study*, *Physical Review Letters* **71**, 2413 (1993).
- [38] A. Goldoni, L. Sangaletti, F. Parmagiani, S. L. Fried- mann, Z.-X. Shen, M. Peloi, G. Comelli, and G. Paolucci, *Phase transition, molecular motions, and inequivalent carbon atoms in K_3C_{60} (111) single-phase ordered films*, *Physical Review B* **59**, 16071 (1999).

- [39] K. Sugihara, T. Inabe, Y. Maruyama, and Y. Achiba, *Thermoelectric Power of Alkali Doped C_{60}* , *Journal of the Physical Society of Japan* **62**, 2757 (1993).
- [40] D. T. Morelli, *Thermoelectric power of superconducting fullerenes*, *Physical Review B* **49**, 655 (1994).
- [41] J. Chang, N. Doiron-Leyraud, O. Cyr-Choinière, G. Grissonnanche, F. Laliberté, E. Hassinger, J.-P. Reid, R. Daou, S. Pyon, T. Takayama, H. Takagi, and L. Taillefer, *Decrease of upper critical field with underdoping in cuprate superconductors*, *Nature Physics* **8**, 751 (2012).
- [42] S. D. Kang and G. J. Snyder, *Charge-transport model for conducting polymers*, *Nature Materials* **16**, 252 (2017).
- [43] K. Michaeli and A. M. Finkel'stein, *Fluctuations of the superconducting order parameter as an origin of the Nernst effect*, *Europhysics Letters* **86**, 27007 (2009).
- [44] M. N. Serbyn, M. A. Skvortsov, A. A. Varlamov, and V. Galitski, *Giant Nernst effect due to fluctuating Cooper pairs in superconductors*, AIP Conference Proceedings **1134**, 140 (2009).
- [45] G. Blatter, M. V. Feigel'man, V. B. Geshkenbein, A. I. Larkin, and V. M. Vinokur, *Vortices in high-temperature superconductors*, *Reviews of Modern Physics* **66**, 1125 (1994).
- [46] V. J. Emery and S. A. Kivelson, *Importance of phase fluctuations in superconductors with small superfluid density*, *Nature* **374**, 434 (1995).
- [47] V. Buntar, F. M. Sauerzopf, and H. W. Weber, *Lower critical fields of alkali-metal-doped fullerene superconductors*, *Physical Review B* **54**, R9651 (1996).
- [48] A. L. Woodcraft and A. Gray, *A low temperature thermal conductivity database*, AIP Conference Proceedings **1185**, 681 (2009).
- [49] O. Klein, G. Grüner, S.-M. Huang, J. B. Wiley, and R. B. Kaner, *Electrical resistivity of K_3C_{60}* , *Physical Review B* **46**, 11247 (1992).